Rotational dynamics of solid C_{70}: A neutron-scattering study

Christos Christides, T. John S. Dennis, and Kosmas Prassides

School of Chemistry and Molecular Sciences, University of Sussex, Brighton BN1 9QJ, United Kingdom

Ronald L. Cappelletti

Department of Physics and Astronomy, Ohio University, Athens, Ohio 45701

D. A. Neumann and J. R. D. Copley

Materials Science and Engineering Laboratory, National Institute of Standards and Technology, Gaithersburg, Maryland 20899

We report the results of neutron-diffraction and low-energy neutron-inelastic-scattering experiments on high-purity solid C_{70} between 10 and 640 K. Thermal hysteresis effects are found to accompany structural changes both on cooling and on heating. The observed diffuse scattering intensity does not change with temperature. At 10 K broad librational peaks are observed at 1.82(16) meV [full width at half maximum = 1.8(5) meV]. The peaks soften and broaden further with increasing temperature. At and above room temperature, they collapse into a single quasielastic line. At 300 K, the diffusive reorientational motion appears to be somewhat anisotropic, becoming less so with increasing temperature. An isotropic rotational diffusion model, in which the motions of adjacent molecules are uncorrelated, describes well the results at 525 K. The temperature dependence of the rotational diffusion constants is consistent with a thermally activated process having an activation energy of 32(7) meV.

I. INTRODUCTION

The high-temperature face-centered cubic (fcc, $Fm\overline{3}m$) phase of solid C_{60} undergoes a first-order phase transition at $T_c = 260$ K to an orientationally ordered simple cubic ($Pa\overline{3}$) phase.[1-4] The molecular dynamics change abruptly at T_c from quasi-isotropic rotational diffusion to "shuffling" between two distinct nearly degenerate orientations, differing in energy by ~ 11.4 meV.[1-7] As yet, a comparable understanding of the structural and dynamical properties of solid C_{70} has not been achieved. Reasons include the relative scarcity of large crystalline samples of sufficient purity and the greater complexity associated with the lower symmetry of the C_{70} molecule. Early x-ray-diffraction and electron-microscopy experiments[8] indicated a greater concentration of defects than in C_{60}, and revealed coexistence of fcc and hexagonal-close-packed (hcp) crystalline phases. Neutron-diffraction measurements on the fcc phase[9] of C_{70} led to the identification of a well-defined transition to a rhombohedral phase with little change in the unit-cell dimension and a rhombohedral angle of $\sim 85.6°$, suggesting that the long molecular axis is aligned along the unit-cell diagonal. This phase must have uniaxial orientational disorder since the long molecular axis has fivefold symmetry, which is incompatible with the $\overline{3}$ symmetry of the unit-cell diagonal. The rhombohedral phase appears on cooling at $\sim 270-280$ K but persists on heating to ~ 340 K.[9] At even lower temperatures, the crystallographic symmetry is found to be lower than rhombohedral. In this case, symmetry considerations allow the molecules to lock into a fully orientationally ordered phase. A more recent high-resolution x-ray-diffraction study[10] established the symmetry of the low-temperature phase as monoclinic but placed the fcc→rhombohedral phase transition at

345 K. Experimental information on the rotational dynamics has come thus far from μSR studies of solid C_{70} in which the muons act as spin labels, sensitive to the motion of the fullerene molecules.[11,12] Reorientational disorder of the long molecular axis sets in gradually at about 160 K on the μSR time scale and a small anisotropy of the motion persists across the ~ 270-K transition into the orientationally disordered fcc phase. Furthermore, information on both the intramolecular[13] (at 20 K) and intermolecular[14] (between 20 and 320 K) excitations of C_{70} has been recently provided by studies employing the neutron time-of-flight technique.

Neutron-inelastic-scattering (NIS) measurements have been successfully used to probe the rotational dynamics of C_{60}. Below the 260-K ordering transition, the observed excitations at nonzero (~ 2.5 meV) energy transfer are due to molecules librating about their equilibrium orientations;[7] as the temperature is raised through T_c the librational excitations collapse, and the appearance of a quasielastic line (i.e., a broad line centered at zero energy transfer) signals the onset of rotational diffusion.[15] In the present work, we employ NIS to study the temperature evolution of the reorientational dynamics of C_{70} between 10 and 640 K. Low-energy librational modes are observed at low T, whereas at high temperatures the observed scattering is better described as quasielastic, due to some sort of rotational diffusion. We have also found that there is substantial diffuse scattering which does not appear to diminish upon cooling through the ordering transition, in sharp contrast to the situation encountered in C_{60}.

II. MATERIALS AND METHODS

The C_{70} powder was separated from C_{60} by alumina column chromatography using hexane as eluent. After

washing with acetone, the solid extract was recrystallized from benzene. It was then sublimed in a high-vacuum system (10^{-6} Torr) at 840 K using a small cylindrical furnace. In all, 500 mg of sublimed C_{70} powder were produced in this way ($\geq 98.5\%$ C_{70}, $\leq 1.5\%$ C_{60}). The final treatment of the sample involved extended annealing at 525 K (≥ 2 days) in sealed quartz tubes.[11,12] This led to a highly crystalline material with no traces of trapped solvent and a clean fcc [$a = 14.931(8)$ Å] x-ray-diffraction profile at room temperature.[9] The sample was further characterized by high-resolution powder neutron diffraction,[9] and by infrared and ^{13}C NMR spectroscopy. An indication of the purity of the present sample came from analysis of its total hydrogen content by prompt gamma-ray neutron-activation analysis;[16] this was determined to be 0.046(7)% by weight, i.e., roughly one H atom for every three C_{70} molecules.

The neutron-scattering measurements were performed at the Neutron Beam Split-Core Reactor (NBSR) at the National Institute of Standards and Technology. Diffraction profiles were recorded at 100 and 300 K using the five-detector high-resolution powder diffractometer BT1 with a wavelength of 1.54 Å. The inelastic-scattering measurements were performed using the BT4 triple-axis spectrometer with fixed incident neutron energies E_i of 28 and 35 meV. The incident neutron beam was monochromated using the Cu(220) reflection and the scattered neutrons were analyzed using the pyrolytic graphite (004) reflection. The measured resolution at the elastic line for 60'-40'-40'-40' collimations was 1.057(9) meV full width at half maximum (FWHM) for $E_i = 28$ meV and 1.57(2) meV for $E_i = 35$ meV. High-resolution diffraction scans were also obtained using the BT4 spectrometer with an incident wavelength of 4.08 Å. For each experiment, the sample was loaded in an aluminum (or a stainless steel) cylindrical can and placed inside a closed-cycle He refrigerator (or a furnace). In the analysis of the inelastic-scattering measurements, background runs were first subtracted, the intensities were corrected for changes in the scattered energy contribution to the spectrometer resolution, and then the spectra were symmetrized. The corrected data were subsequently fitted using a δ function at zero energy transfer ($\hbar\omega = 0$) and Lorentzians centered either at zero or nonzero energy transfer, each convoluted with the measured Gaussian instrumental resolution function.

III. NEUTRON DIFFRACTION

In Fig. 1 we show neutron-diffraction profiles at 100 and 300 K, obtained using the BT1 spectrometer. Both spectra are dominated by Bragg scattering at low values of the scattering vector Q and by continuous diffuse scattering at high Q. However, the Bragg peak intensities at low Q are considerably reduced on cooling to 100 K, while their widths increase, suggestive of partially resolved peak splittings. This implies a change to a lower symmetry crystal structure.[9,10] This is further confirmed by the higher-resolution 4.08 Å measurements shown in Fig. 2. Before cooling (bottom panel), a clean profile that can be indexed as fcc is observed at room temperature,

but the low T (11 K) data are clearly more complicated with peaks apparently broader than the instrumental resolution. These results are consistent with earlier diffraction studies[9,10] that established the existence of phase transitions to rhombohedral and monoclinic phases on cooling. What is also noteworthy is that the 11-K profile includes a peak at 1.2 $Å^{-1}$ which is absent in the rhombohedral and monoclinic phases[9,10] and must therefore be the (220) fcc reflection. Thus, a fraction of the high-temperature fcc phase appears to persist even at the lowest temperature of the present experiment, implying severe hysteresis effects. Furthermore the position of the (220) reflection implies a rather large increase of $\sim 0.8\%$ in the cubic lattice constant between 11 and 300 K, identical to the one observed in solid C_{60}.[3,6] Hysteresis effects are also evident in the room-temperature profile, recorded on heating (Fig. 2, middle panel). While the intensities of the fcc peaks have increased substantially, a fraction of the rhombohedral phase is still present at room temperature, only disappearing on further heating to ~ 350 K.[9] The rhombohedral/fcc transition is thus already underway well below the 345-K transition observed in the sample of Ref. 10. Coexistence of the fcc and simple cubic phases of C_{60} has also been observed,[6,17] albeit over a temperature range of ~ 5 K.[17] This does not necessarily violate the Gibbs rule, which, for a single-component sys-
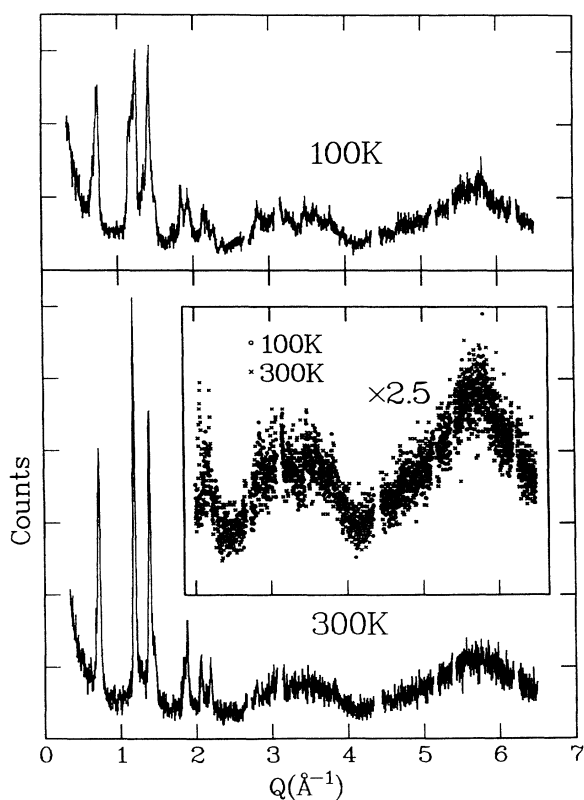
FIG. 1, Diffraction profiles of C_{70} at 100 and 300 K, measured with 1.54-Å neutrons. The profiles are normalized to the same monitor count. Gaps represent the positions of lines due to the aluminum sample holder. In the inset, data at the two temperatures between 2 and 6.5 $Å^{-1}$ are superimposed.

tem, forbids the coexistence of two phases over a range of temperature in the absence of an applied field; the large stresses which accompany the transition could provide the required field.

In the inset of Fig. 1 we show superimposed diffraction profiles in the Q-range 2–6.5 Å^{-1} at 100 and 300 K. Both the shape and the magnitude of the diffuse scattering change very little with temperature. A possible explanation for the low-temperature diffuse scattering is substantial static disorder arising from frozen-in "misorientations" of the molecules. The resulting defects and microstrains are presumably responsible for the observed hysteresis effects described above. Furthermore, anisotropic (uniaxial) motion persists to low temperatures,[11,12] resulting in additional dynamic (orientational) disorder and a featureless diffraction profile at $Q > 3$ Å^{-1}. This is in sharp contrast to the situation encountered in C60, where the observed diffuse scattering is considerably reduced in intensity below the 260-K ordering transition.[4] An alternative description for the continuous scattering at low temperature is that it is Bragg peaks
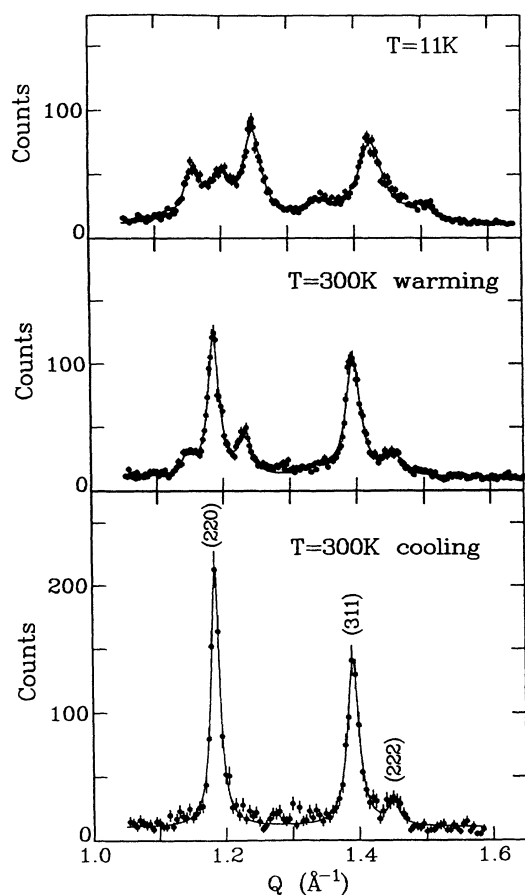
that have been considerably strain broadened by the stresses that accompany the transitions.

IV. NEUTRON INELASTIC SCATTERING

In order to study the rotational motion of the molecules in solid C70, we have performed detailed NIS measurements, at several temperatures, as a function of Q and ω. Figures 3(a)–3(d) show representative spectra at temperatures between 100 and 640 K with $Q = 5.6$ Å^{-1}. In each case the points are the corrected data, the solid line is a fit of the type described in Sec. II, and the dashed lines show Lorentzian components of the fit. At 100 and 200 K, fits with Lorentzians at nonzero energy transfer
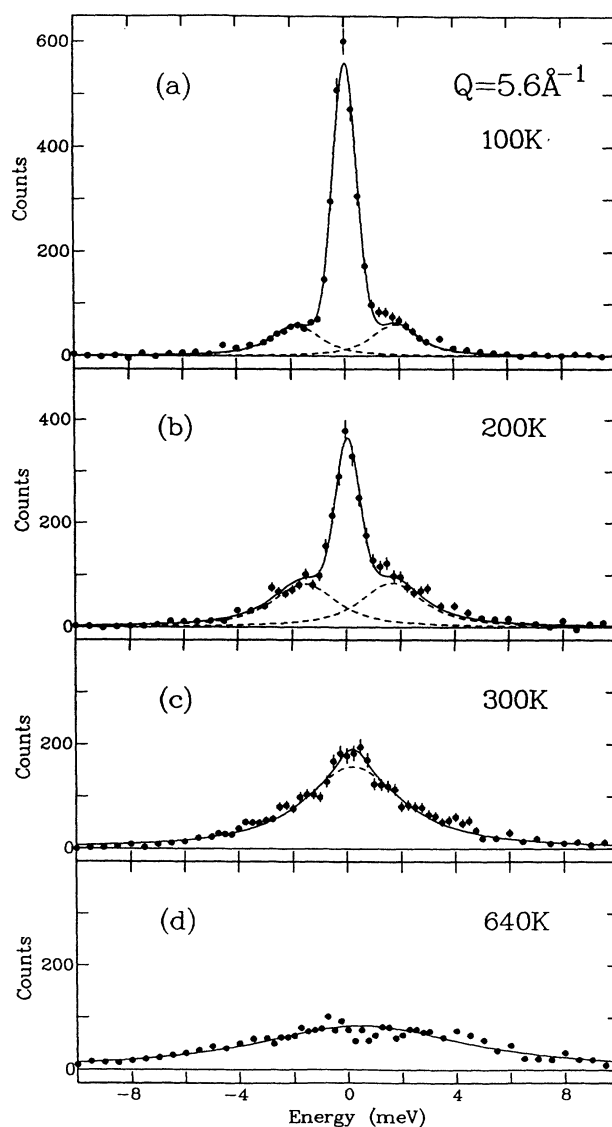

FIG. 2. Diffraction profiles of C70, over a limited range of Q, measured with 4.08-Å neutrons. The top panel shows the pattern at 11 K. The middle panel shows the pattern at 300 K on warming. The bottom panel shows the pattern at 300 K before cooling. The solid line is a fit using Lorentzians. Note that the peaks at 11 K are considerably broader than the instrumental resolution.

FIG. 3. Representative neutron-inelastic-scattering spectra at constant $Q = 5.6$ Å^{-1}. (a) $T = 100$ K, (b) $T = 200$ K, (c) $T = 300$ K, and (d) $T = 640$ K. The solid circles are experimental points and the solid lines are best fits, as discussed in the text. The dashed lines show the individual Lorentzian components of the fits.

were generally superior to fits with a single Lorentzian at $\hbar\omega = 0$. On the other hand, fits to the higher-temperature spectra with Lorentzians at $\hbar\omega \neq 0$ were unsuccessful; the Lorentzians collapsed to a single central line. At all temperatures the Q dependence of the energy-integrated scattering intensity implies that the observed scattering is due to rotational motion of the molecules.[4,7,18] Thus, librational behavior occurs at temperatures below the orientational ordering transition [Figs. 3(a) and 3(b)], whereas we find no evidence for this type of motion at and above room temperature [Figs. 3(c) and 3(d)]. Instead, the higher-temperature spectra are well described at all Q by a quasielastic component which is much broader than the instrumental resolution, suggesting that fullerene molecules are undergoing some form of rotational diffusion at these temperatures. It is also evident from Fig. 3 that the intensity of the elastic component of the scattering decreases with increasing temperature. On the other hand, the energy-integrated intensity is essentially independent of temperature, consistent with our previous observation that the diffracted intensity in this Q range does not also change with temperature. Together, these results suggest that a rotational diffusion component of the motion may persist on time scales longer than those observable with the energy resolution of the present measurements.

A. Low-temperature results

Figures 4(a) and 4(b) show the temperature dependence of the energy and full width of the librational modes, as extracted from the fits. Our results agree well with those of Renker *et al.*,[14] except that their full width at 250 K is somewhat smaller than ours. Comparative results for C_{60} (Ref. 7) are also shown in Fig. 4; there are smaller error bars on the C_{60} results because the peaks in the spectra are more clearly separated than in C_{70}. The low-temperature librational energy in C_{70} [1.82(16) meV at 10 K] is much lower than in C_{60} [2.77(6) meV at 20 K], and the softening of the mode between 10–20 and 250 K is significantly smaller in C_{70} ($\sim 17\%$) than in C_{60} ($\sim 35\%$). Furthermore, the observed full widths are substantially larger in C_{70} than in C_{60} [1.8(5) and 0.38(18) meV at 10 and 20 K, respectively], and they change less with temperature. The difference in moments of inertia between C_{60} ($I = 1.0 \times 10^{-43}$ kg m^2) and C_{70} ($I_{\parallel} = 1.24 \times 10^{-43}$ and $I_{\perp} = 1.44 \times 10^{-43}$ kg m^2) is insufficient to explain the difference in the observed low-temperature librational energies, and the difference in the moments of inertia of the C_{70} molecule about axes parallel ($I_{\parallel}$) and perpendicular ($I_{\perp}$) to the fivefold axis does not by itself account for the observed widths. Our conclusion is that the orientational potential is softer and more anisotropic for C_{70} than for C_{60}. Additional broadening may be due to increased dispersion associated with the lower-symmetry crystal structure of solid C_{70} at low temperatures. To further address these questions, measurements on single crystals are required.

The experimental results can be compared directly to molecular-dynamics calculations, providing a stringent test of various interatomic potentials. For instance,
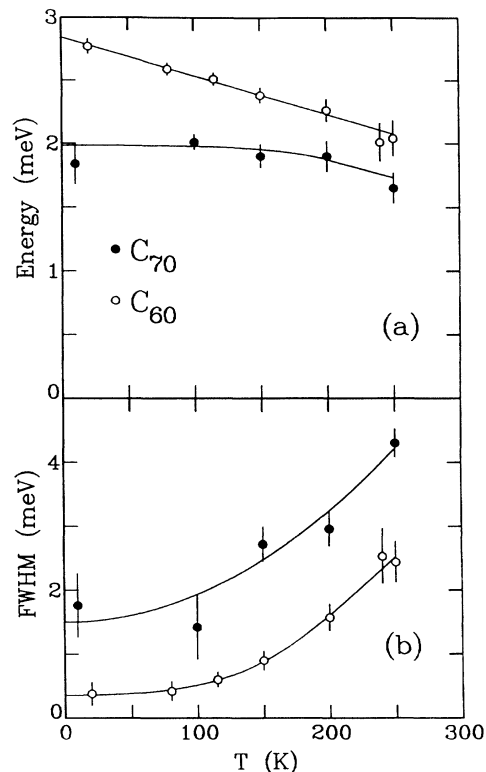

FIG. 4. Temperature dependence of (a) the librational energy, and (b) the full width of the librational peaks. Lines are guides to the eyes. Earlier results for C_{60} (Ref. 7) are included for comparison.

Cheng and Klein[19] have modeled the intermolecular C-C interactions using a standard Lennard-Jones potential with $\varepsilon = 28$ K and $\sigma = 3.4$ Å. Their calculation results in a librational density of states which peaks at ~ 1.2 meV and has a width of 0.9 meV, both considerably less than the experimental values. This indicates a model orienta-
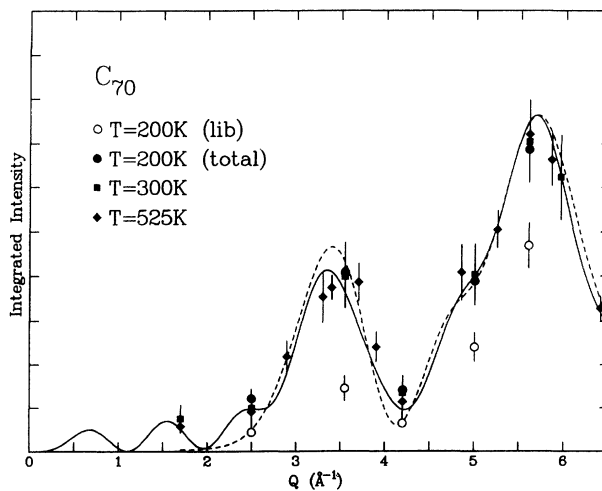

FIG. 5. Q dependence of the intensity of the quasielastic scattering at 525 and 300 K and of both the total integrated intensity and the intensity of the librational peaks at 200 K. The solid (dashed) line is the calculation for uncorrelated isotropic (uniaxial) rotational diffusion of C_{70} molecules. Both calculations are scaled to have the same intensity at $Q = 5.7$ Å^{-1}.

tional potential softer by a factor of 2 than the one required by experiment, reminiscent of the situation in C$_{60}$ (Refs. 7 and 20) where the calculated orientational potential was too small by a factor of 4. The greater deviation between model calculations and experiment in C$_{60}$ arises from the additional anisotropic contributions to the orientational potential associated with the nesting of the short bonds in the pentagons (or hexagons) of adjacent molecules.[21]

At fixed Q, the integrated intensity of the low-energy librational modes increases smoothly with temperature, consistent with harmonic behavior. On the other hand, the Q dependence of the integrated intensity at fixed temperature has the characteristic shape (Fig. 5) that we associate with rotational motion by analogy with previous results for C$_{60}$.[4,7,15] Presumably, the orientational order-disorder transition occurs, as in C$_{60}$, when librational amplitudes become sufficiently large to sample a substantial fraction of the near-neighbor interatomic angles.

B. High-temperature results

At 300 K and above, quasielastic scattering is observed. Plots of the Q dependence of the integrated intensities at 300 and 525 K are shown in Fig. 5. The observed behavior is again reminiscent of the situation in C$_{60}$.

We have calculated the coherent scattering function assuming a model in which each C$_{70}$ molecule undergoes random-walk anisotropic rotational diffusion with diffusion-constant components $D_{\parallel}$ and $D_{\perp}$, parallel and perpendicular to a fixed molecular axis. The rotational motion of each molecule is assumed to be uncoupled from its translational motion, and the rotations of neighboring molecules are assumed to be uncorrelated. The *incoherent* neutron-scattering law was first evaluated for such a model by Zeidler.[22] For coherent scatterers such as carbon, the geometry of the diffusing molecule has to be taken into account in calculating the powder-averaged rotational component of the coherent neutron-scattering function $S_R(Q,\omega)$, which is expressed as a sum of Lorentzian functions as

$$S_R(Q,\omega)= \sum_{l=1}^{\infty} \sum_{m=-l}^{+l} S_{lm} \frac{1}{\pi} \frac{\tau_{lm}}{1+\omega^2\tau_{lm}^2} . \qquad (1)$$

Here,

$$S_{lm}=4\pi \left| \sum_{v=1}^{70} j_l(QR_v)Y_{lm}(\hat{R_v}) \right|^2 , \qquad (2)$$

$$\tau_{lm}^{-1}=\tau_l^{-1}+\tau_m^{-1}, \quad \tau_l^{-1}=l(l+1)D_{\perp} ,$$
$$\tau_m^{-1}=m^2(D_{\parallel}-D_{\perp}) , \qquad (3)$$

j_l are spherical Bessel functions, $Y_{lm}(\hat{R_v})$ are spherical harmonics, and $R_v(\hat{R_v})$ specify the magnitude (direction) of the vector $\mathbf{R}_v$ that joins atom v to its molecular center. In our calculations, the coordinates of atoms in the C$_{70}$ molecule were taken from Ref. 23.

Our model, described by Eqs. (1)–(3), reduces to the full isotropic case by setting $D_{\perp}=D_{\parallel}\equiv D_r$. This type of

model has been successfully applied to describe the rotational motion of C$_{60}$ in its plastic phase.[4,15] In the present case, the Q dependence of the integrated intensity of the quasielastic scattering, calculated using such an isotropic diffusion formalism, is shown in Fig. 5 as the solid line. A detailed comparison of the experimental measurements with the calculated spectra convoluted with the instrumental resolution, assuming a rotational diffusion constant $D_r=1.5\times10^{10}$ s^{-1} [cf. D_r (C$_{60}$, 520 K)$=2.8\times10^{10}$ s^{-1}] is shown in Fig. 6. Note that the only two parameters in this comparison are an overall scale factor and D_r. In selecting a value for the diffusion constant, we relied on fitting the *complete line shape* rather than on fitting simply the full width of the quasielastic line. Clearly there is good, though not perfect, agreement between our 525-K data and the isotropic diffusion model, implying that at this temperature the C$_{70}$ molecules sample all orientations with essentially equal probability, thereby averaging over the anisotropy of the molecule. Reorientational motions of individual molecules at this temperature are thus effectively random with no pronounced intermolecular correlations. It should be noted, however, that the polycrystalline nature of the sample will tend to mask any possible correlations or small anisotropy in the motion.

At 300 K the agreement between the measured spectra and the isotropic diffusion model calculation is not as
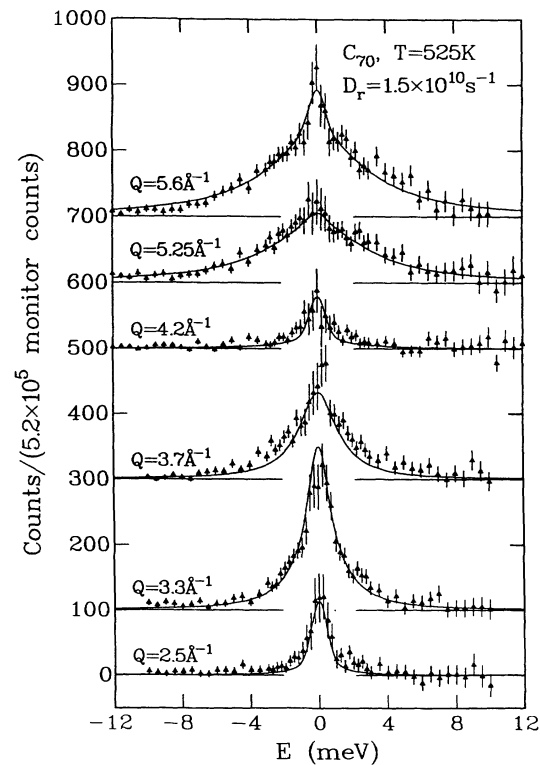

FIG. 6. Neutron-inelastic-scattering spectra taken at several values of Q at 525 K, normalized to the same total monitor count. The solid lines are the calculated spectra convoluted with the instrumental resolution using an isotropic diffusion constant of $D_r=1.5\times10^{10}$ s^{-1}. Note that the only two parameters in this comparison are an overall scale factor and D_r.

good. In this case, a detailed comparison of the experimental measurements with the calculated spectra, assuming an isotropic diffusion constant $D_r = 1.0 \times 10^{10}$ s^{-1} [cf. D_r (C_{60}, 260 K) $= 1.4 \times 10^{10}$ s^{-1}] is shown in Fig. 7. The criterion for selecting a value for D_r was the same as for the 525-K data. At 300 K, the isotropic model is somewhat less satisfactory in describing the experimental data. This is consistent with the μSR experimental results,[12] which indicate that there is anisotropy in the molecular motion at this temperature.

The shape of the C_{70} molecule necessitates that diffusion about the long symmetry axis should occur at a different rate than that of diffusion of the symmetry axis itself. Setting $D_{\parallel} \equiv D_r^u$ and $D_{\perp} = 0$ in Eqs. (1)–(3) leads to a model for the rotational dynamics of C_{70} in which each individual molecule performs diffusive motion *only* about a fixed molecular axis (which may or may not coincide with the long axis). Equations (1)–(3) then simplify to read[14]

$$S_R(Q,\omega) = \sum_{m=1}^{\infty} S_m \frac{1}{\pi} \frac{\tau_m}{1 + \omega^2 \tau_m^2} , \qquad (4)$$

with

$$S_m = (8\pi) \sum_{n=m}^{\infty} \left| \sum_{\nu=1}^{70} j_n(QR_\nu) Y_{nm}(\hat{R}_\nu) \right|^2 , \qquad (5)$$

and

$$\tau_m^{-1} = m^2 D_r^u . \qquad (6)$$

Equation (5) corrects a typographical error which appeared before in an equivalent expression by Renker *et al.*[14] If the fixed rotation axis is taken to coincide with the fivefold axis of the molecule, S_m is only nonzero when m is an integral multiple of 5. For $Q \leq 6.5$ Å^{-1}, contributions from terms with $m > 25$ are essentially negligible. An expression equivalent to Eq. (5), which was actually used in comparing the model to data, and which converges rapidly in computations, can be derived using cylindrical coordinates:

$$S_m = \sum_{\nu,\nu'=1}^{70} \cos(m\phi_{\nu\nu'})$$

$$\times \int_0^\pi d\Theta \sin\Theta \cos[Q \cos\Theta(z_\nu - z_{\nu'})]$$

$$\times J_m(Qr_\nu \sin\Theta) J_m(Qr_{\nu'} \sin\Theta) . \qquad (7)$$

In this expression, z_ν is the projection of the position vector R_ν along the fixed molecular axis (which without loss of generality lies along the z direction), r_ν is its projection on the equatorial plane, and $\phi_{\nu\nu'}$ is the azimuthal angle between the position vectors $R_\nu, R_{\nu'}$ of atoms ν and ν' within the same molecule. Furthermore Θ is the angle between the scattering vector Q and the z axis, and J_m are cylindrical Bessel functions of integer order m.

The dashed line in Fig. 5 shows a calculation of the quasielastic integrated intensity using the uniaxial diffusion model. A detailed comparison between the two models (uniaxial with $D_r^u = 4.0 \times 10^{10}$ s^{-1} and isotropic with $D_r = 1.0 \times 10^{10}$ s^{-1}) and the experimental NIS data

at 300 K is shown in Fig. 7; the uniaxial model does not describe the experimental data as well as the isotropic model. Discrepancies between the isotropic model predictions and the experimental measurements would perhaps be removed with the introduction of a small anisotropy in the reorientational motion (i.e., considering two slightly different diffusion constants $D_{\parallel}$ and $D_{\perp}$), as necessitated by the μSR results.[12] However, the present data do not warrant the introduction of a second diffusion parameter. We also note that our conclusion here is at variance with the earlier work of Ref. 14. Those authors concluded that the uniaxial model appears to be superior to the isotropic one at 320 K; this was based on comparisons of the full widths of the quasielastic peaks with values extracted from fitting the calculated spectra with single Lorentzians. However, the single-Lorentzian-peak description is invalid for Q greater than ~ 3 Å^{-1}, yielding essentially misleading conclusions if comparisons are made between experiment and calculation on the basis of peak widths alone, as revealed by our own measurements which were performed with much higher resolution in Q. Moreover, the C_{70} sample of Ref. 14 was a mixture of fcc and hcp phases at the tempera-
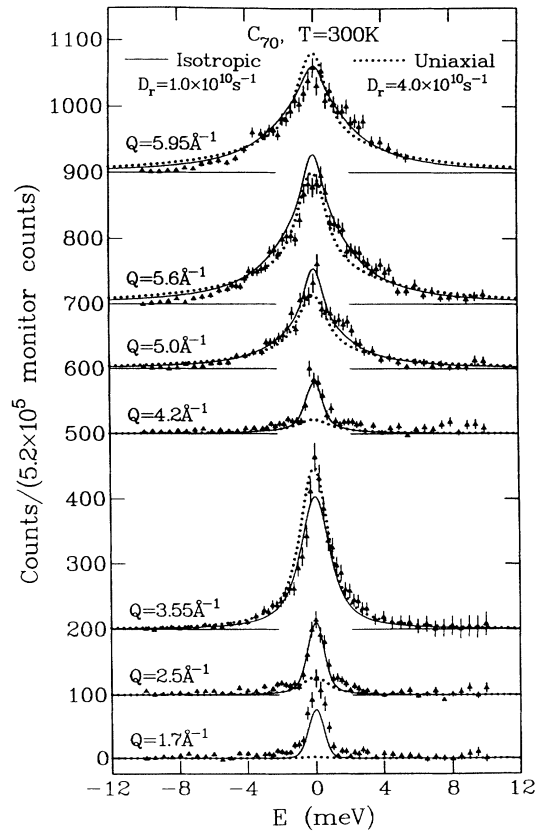

FIG. 7. Neutron-inelastic-scattering spectra taken at several values of Q at 300 K, normalized to the same total monitor count. The solid (dashed) lines are the calculated spectra convoluted with the instrumental resolution using an isotropic (uniaxial) diffusion constant of $D_r = 1.0 \times 10^{10}$ s^{-1} ($D_r^u = 4.0 \times 10^{10}$ s^{-1}). Note that the only two parameters in this comparison are an overall scale factor and D_r.

tures of measurement.

NIS measurements were also performed at a series of temperatures between 300 and 640 K at $Q = 5.6$ Å^{-1}. The observed temperature dependence of the isotropic diffusion constant is consistent with a thermally activated process having an activation energy of 32(7) meV. This is comparable to the corresponding activation energy for C_{60} of 35(15) meV.[4,15]

V. CONCLUSION

We have measured neutron-diffraction profiles at temperatures between 10 and 300 K, and low-energy NIS spectra of solid C_{70} as a function of scattering vector, at various temperatures between 10 and 640 K. The sample was fcc at room temperature, transforming to a lower-symmetry structure on cooling. Severe thermal hysteresis effects are found to accompany the structural changes. The intensity of the diffuse scattering does not change appreciably with temperature. At 250 K and below, the fullerene molecules librate about their equilibrium positions, giving rise to NIS peaks near 2 meV. The librational energy is smaller than in C_{60} and the peaks are much broader, reflecting a weaker and more anisotropic orientational potential. The librations soften and their amplitudes increase as the temperature increases until the librational peaks collapse into a single quasielastic line at 300 K and above. At 300 K an isotropic diffusion model is in better agreement with the data than a uniaxial model. Remaining discrepancies may be reduced by including an anisotropic contribution in the model. Increasing the temperature leads to faster tumbling of the C_{70} molecules and the quasielastic data at 525 K are in good agreement with the isotropic rotational-diffusion model. The high-temperature rotational motion is found to be thermally activated with an activation barrier of 32(7) meV.

[1]P. A. Heiney, J. Phys. Chem. Solids **53**, 1333 (1992).

[2]R. D. Johnson, D. S. Bethune, and C. S. Yannoni, Acc. Chem. Res. **25**, 169 (1992).

[3]K. Prassides, H. W. Kroto, R. Taylor, D. R. M. Walton, W. I. F. David, J. Tomkinson, M. J. Rosseinsky, D. W. Murphy, and C. R. Haddon, Carbon **30**, 1277 (1992).

[4]J. R. D. Copley, D. A. Neumann, R. L. Cappelletti, and W. A. Kamitakahara, J. Phys. Chem. Solids **53**, 1353 (1992).

[5]R. Tycko, G. Dabbagh, R. M. Fleming, R. C. Haddon, A. V. Makhija, and S. M. Zahurak, Phys. Rev. Lett. **67**, 1886 (1991); R. D. Johnson, C. S. Yannoni, H. C. Dorn, J. R. Salem, and D. S. Bethune, Science **255**, 1235 (1992).

[6]W. I. F. David, R. M. Ibberson, T. J. S. Dennis, J. P. Hare, and K. Prassides, Europhys. Lett. **18**, 219 (1992); **18**, 735 (1992).

[7]D. A. Neumann, J. R. D. Copley, W. A. Kamitakahara, J. J. Rush, R. L. Cappelletti, W. J. Romanow, N. Coustel, J. P. McCauley, J. E. Fischer, A. B. Smith, K. M. Creegan, and D. M. Cox, J. Chem. Phys. **96**, 8631 (1992).

[8]G. B. M. Vaughan, P. A. Heiney, J. E. Fischer, D. E. Luzzi, D. A. Ricketts-Foot, A. R. McGhie, Y.-W. Hui, A. L. Smith, D. E. Cox, W. J. Romanow, B. H. Allen, N. Coustel, J. P. McCauley, and A. B. Smith, Science **254**, 1350 (1992).

[9]C. Christides, I. M. Thomas, T. J. S. Dennis, and K. Prassides, Europhys. Lett. **22**, 611 (1993).

[10]G. B. M. Vaughan, P. A. Heiney, D. E. Cox, J. E. Fischer, A. R. McGhie, A. L. Smith, R. M. Strongin, M. A. Cichy, and A. B. Smith (unpublished).

[11]K. Prassides, T. J. S. Dennis, C. Christides, E. Roduner, H. W. Kroto, R. Taylor, and D. R. M. Walton, J. Phys. Chem. **96**, 10 600 (1992).

[12]T. J. S. Dennis, K. Prassides, E. Roduner, L. Cristofolini, and R. DeRenzi, J. Phys. Chem. **97**, 8553 (1993).

[13]C. Christides, A. V. Nikolaev, T. J. S. Dennis, K. Prassides, F. Negri, G. Orlandi, and F. Zerbetto, J. Phys. Chem. **97**, 3641 (1993).

[14]B. Renker, F. Gompf, R. Heid, P. Adelmann, A. Heiming, W. Reichardt, G. Roth, H. Schober, and H. Rietschel, Z. Phys. B **90**, 325 (1993).

[15]D. A. Neumann, J. R. D. Copley, R. L. Cappelletti, W. A. Kamitakahara, R. M. Lindstrom, K. M. Creegan, D. M. Cox, W. J. Romanow, N. Coustel, J. P. McCauley, N. C. Maliszewskyj, J. E. Fischer, and A. B. Smith, Phys. Rev. Lett. **67**, 3808 (1991).

[16]M. P. Failey, D. L. Anderson, W. H. Zoller, G. E. Gordon, and R. M. Lindstrom, Anal. Chem. **51**, 2209 (1979).

[17]P. A. Heiney, G. B. M. Vaughan, J. E. Fischer, N. Coustel, D. E. Cox, J. R. D. Copley, D. A. Neumann, W. A. Kamitakahara, K. M. Creegan, D. M. Cox, J. P. McCauley, and A. B. Smith, Phys. Rev. B **45**, 4544 (1992).

[18]C. Christides, D. A. Neumann, K. Prassides, J. R. D. Copley, J. J. Rush, M. J. Rosseinsky, D. W. Murphy, and R. C. Haddon, Phys. Rev. B **46**, 12 088 (1992).

[19]A. Cheng and M. L. Klein, Phys. Rev. B **46**, 4958 (1992).

[20]A. Cheng and M. L. Klein, Phys. Rev. B **45**, 1889 (1992).

[21]W. I. F. David, R. M. Ibberson, J. C. Matthewman, K. Prassides, T. J. S. Dennis, J. P. Hare, H. W. Kroto, R. Taylor, and D. R. M. Walton, Nature **353**, 147 (1991).

[22]M. D. Zeidler, Ber. Bunsenges. Physik, Chem. **75**, 769 (1971).

[23]J. Baker, P. W. Fowler, P. Lazzeretti, M. Malagoli, and R. Zanasi, Chem. Phys. Lett. **184**, 182 (1991).